6208–6224 *Nucleic Acids Research, 2019, Vol. 47, No. 12* *Published online 13 May 2019*
doi: 10.1093/nar/gkz376

Chromatin remodeler Ep400 ensures oligodendrocyte survival and is required for myelination in the vertebrate central nervous system

Olga Elsesser[1,†], Franziska Fröb[1,†], Melanie Küspert[1], Ernst R. Tamm[2], Toshihiro Fujii[3], Rikiro Fukunaga[3] and Michael Wegner[1,*]

[1]Institut für Biochemie, Emil-Fischer-Zentrum, Friedrich-Alexander-Universität Erlangen-Nürnberg, Erlangen, Germany, [2]Institut für Humananatomie und Embryologie, Universität Regensburg, Regensburg, Germany and [3]Department of Biochemistry, Osaka University of Pharmaceutical Sciences, Osaka, Japan

Received October 10, 2018; Revised April 26, 2019; Editorial Decision April 29, 2019; Accepted May 02, 2019

ABSTRACT

Differentiating oligodendrocytes generate myelin to ensure rapid saltatory conduction in the vertebrate central nervous system. Although oligodendroglial differentiation and myelination are accompanied by dramatic chromatin reorganizations, previously studied chromatin remodelers had only limited direct effects on the process. To study the functional significance of chromatin changes for myelination and identify relevant remodelers, we deleted *Ep400*, the central ATP-hydrolyzing subunit of the TIP60/EP400 complex, at defined times of mouse oligodendrocyte development. Whereas Ep400-deficient oligodendrocyte precursors develop normally, terminal differentiation and myelination are dramatically impaired. Mechanistically, Ep400 interacts with transcription factor Sox10, binds to regulatory regions of the *Myrf* gene and is required to induce this central transcriptional regulator of the myelination program. In addition to reduced and aberrant myelin formation, oligodendrocytes exhibit increased DNA damage and apoptosis so that numbers never reach wildtype levels during the short lifespan of Ep400-deficient mice. Ep400 deletion in already mature oligodendrocytes remains phenotypically inapparent arguing that Ep400 is dispensable for myelin maintenance. Given its essential function in myelin formation, modulation of Ep400 activity may be beneficial in conditions such as multiple sclerosis where this process is compromised.

INTRODUCTION

Oligodendrocytes (OLs) are an evolutionary late addition to the cell repertoire of the vertebrate central nervous system (CNS), specialized in the production of myelin sheaths around axons to allow saltatory conduction of action potentials and thereby optimize information processing. Similar to neurons and astrocytes, OLs are generated from neuroepithelial precursor cells in the ventricular zone. After specification they remain mitotically active and highly migratory as oligodendrocyte precursor cells (OPCs) and eventually differentiate into myelin-forming OLs.

Specification, lineage progression and especially terminal differentiation require dramatic changes in gene expression that are tightly regulated by a unique gene regulatory network whose major components include among other transcription factors the bHLH proteins Olig2, Olig1 and Ascl1, the HMG-domain proteins Sox10 and Tcf7l2, the homeodomain protein Nkx2.2 and the Ntd80-domain protein Myrf (1). Cell-specific regulatory networks have to work within the confines of the existing chromatin landscape or may change it during the course of their action by interacting with a series of epigenetically active factors and complexes with chromatin-modifying functions (2). Among them, ATP-dependent chromatin remodelers are particularly important as they use energy from ATP hydrolysis to change type, position and local density of nucleosomes and thereby alter chromatin structure (3). Many ATP-dependent chromatin remodeling complexes have been identified and are commonly classified by sequence homology of the central ATP-hydrolyzing subunit into four subfamilies. These include the SWI/SNF, the CHD, the INO80/SWR and the ISWI subfamily (4).

*To whom correspondence should be addressed. Tel: +49 9131 85 24620; Email: michael.wegner@fau.de
†The authors wish it to be known that, in their opinion, the first two authors should be regarded as Joint First Authors.

The overall relevance of these chromatin remodelers for oligodendroglial development has been established in mice. By conditional deletion of *Brg1* as the central ATP-hydrolyzing subunit of the BAF complex, this SWI/SNF-type remodeler has been shown to have a dramatic impact on oligodendroglial specification and as a consequence on all following stages (5–7). In contrast, direct effects on OL terminal differentiation and myelination were less pronounced. Recently, conditional deletion of *Chd7* and *Chd8* has identified CHD-type remodelers as additional major contributors to oligodendroglial specification as well as OPC identity, proliferation and survival (8–11). Again, direct influences on terminal differentiation and myelination were limited. Chd7 has been reported to cooperate with Sox10 in influencing the expression of genes that are important for the initiation of myelinogenesis and oligodendroglial maturation (8). However, the effects of Chd7 deletion on OL differentiation were substantially milder than those of Sox10 deletion and transient rather than permanent. Taken together, the analyzed chromatin remodeling activities cannot be solely responsible for the massive chromatin changes that take place in particular during OL differentiation (12). Further considering that the known chromatin remodeling activities appear to be active in the same pathway and act in a cascade-like fashion with Chd8-containing remodelers involved in Brg1 induction and the Brg1-containing BAF complex involved in Chd7 induction (8,11), it is reasonable to assume that major chromatin remodeling activities for OL differentiation have not yet been defined and that they likely belong to separate pathways.

Chromatin remodelers of the INO80/SWR subfamily belong to such a separate pathway and have not been investigated in oligodendroglial development. Therefore we chose to study the role of Ep400, the central ATP-hydrolyzing subunit of the TIP60/EP400 complex (2,3). TIP60/EP400 and other SWR-type complexes are thought to exchange H2A against H2A.Z in nucleosomes preferentially in gene regulatory regions such as the promoter (13–15) and influence gene expression and DNA repair (16). Ep400 has been shown to be essential for renewal and pluripotency in ES cell culture (17) and proper cell-cycle progression in cultured mouse embryonic fibroblasts (18). *In vivo* data on the role of Ep400 are sparse and restricted to the hematopoietic system where Ep400 has been implicated in both embryonic and adult hematopoiesis with increased rates of apoptosis in Ep400-deficient hematopoietic cells before and after lineage commitment (18,19).

Here, we show that Ep400 is dispensable for oligodendroglial specification and lineage progression in mice during embryogenesis but becomes functionally important with the onset of OL differentiation around the time of birth. Loss of Ep400 leads to severe and persistent hypomyelination of the CNS. Additionally, Ep400-deficient OLs exhibit increased DNA damage and apoptosis. This indicates that chromatin changes are essential for successful OL differentiation and that the TIP60/EP400 remodeling complex is a substantial contributor to these changes. Because of its role as a pro-differentiation and survival factor, Ep400 may represent a promising therapeutic target in demyelinating diseases such as multiple sclerosis.

MATERIALS AND METHODS

Transgenic mice and FACS

The *Ep400*$^{fl/fl}$ mouse strain (RBRC03987) was provided via RIKEN BRC through the National Bio-Resource Project of MEXT, Japan. To delete Ep400 at different stages of oligodendroglial development, floxed alleles for *Ep400* (18) were combined in mice with a *Nestin::Cre* transgene (20), a *Sox10::Cre* Bac transgene (21,22), the *Cnp1*^{Cre} allele (23) or the *Mog*$^{i\text{-}Cre}$ (24) allele to yield *Ep400ΔN*, *Ep400ΔS*, *Ep400ΔC* and *Ep400ΔM* mice. In some mice, a floxed allele for *Brg1* (25) or the *Rosa26*$^{stopflox YFP}$ (26) was additionally crossed in. Genotyping was as described (18,20–23,25,26). Transgenic and control mice were on a mixed C3H × C57Bl/6J background and kept under standard housing conditions with 12:12 hours light-dark cycles and continuous access to food and water. For EdU labeling, mice were injected intraperitoneally with 100 μg EdU (Invitrogen, #A10044) per gram body weight 24 h before tissue preparation. Spinal cord and brain tissue were obtained before birth at E12.5, E14.5 and E18.5 and after birth at P1, P6, P14, P32 and P60 from male and female mice with relevant genotypes. Housing and experiments were in accordance with animal welfare laws and approved by the responsible local committees and government bodies (Veterinäramt Stadt Erlangen, Regierung von Unterfranken).

Spinal cord tissue from control and *Ep400*$^{fl/fl}$ mice additionally carrying *Cnp1*^{Cre} and *Rosa26*$^{stopflox YFP}$ alleles was also used at P6 for FACS. After tissue isolation and digestion with DNase I and papain, dissociation to single cells was performed. Cells were stained with Hoechst33342 (Sigma-Aldrich, #B2261, 1:5000 dilution) and passed through a 40 μm cell strainer (Greiner bio-one, #542040). Between 10^7 and 10^8 cells were subjected to FACS on a MoFlo cell sorter (Beckman Coulter) using YFP autofluorescence and Hoechst staining. The resulting 5–10% sorted YFP and Hoechst33342 double-positive cells displayed a purity of 92–98% in re-analysis.

Primary cell culture

Primary oligodendroglial cells were obtained from brain tissue of 6-day-old mice or newborn Wistar rats of both sexes after growth in mixed glial cultures by shake-off (27). For proliferation, rat OPCs were grown on poly-ornithine in N2-supplemented medium containing 10 ng/ml PDGF-AA and 10 ng/ml Fgf2. Mouse OPCs were grown on poly-D-lysine and laminin in the same medium. For differentiation of rat OLs, growth factor containing medium was replaced by SATO medium and 1% FCS. For differentiation of mouse OLs, growth factors were replaced by 1% FCS. For ectopic Myrf expression, mouse OPCs were transduced with a Myrf-containing retrovirus at a MOI of 1, and proliferation medium was changed to differentiation medium 2 days later. Cells were either stained after fixation or used for preparation of whole cell protein extracts or chromatin.

Immunohistochemistry and *in situ* hybridization

Immunohistochemistry and *in situ* hybridization were performed on 10 μm cryotome sections of mouse spinal cord

(forelimb level) or forebrain (hippocampal level). Before sectioning, tissue underwent fixation in 4% paraformaldehyde, dehydration in 30% sucrose and freezing in Tissue Freezing Medium (Leica) (28). Sectioning was followed by *in situ* hybridization with DIG-labeled antisense riboprobes specific for *Mbp* and *Plp1* (28) or immunohistochemistry using the following primary antibodies: rat anti-Mbp monoclonal (Bio-Rad, #MCA409S, Lot #210610, 1:500 dilution), mouse anti-Nkx2.2 monoclonal (Developmental Studies Hybridoma Bank, University of Iowa, clone 74.5A5, 1:5000 dilution), mouse anti-NeuN monoclonal (Chemicon, #MAB377, Lot#19040027, 1:500 dilution), mouse anti-CC1 monoclonal (Calbiochem, #OP80, Lot#D00050836, 1:1000 dilution), guinea pig anti-Sox10 antiserum (home-made, validated on control and knockout mouse tissue, 1:1000 dilution) (29), rabbit anti-Gfap monoclonal (Neomarkers, #RB-087-A, Lot#087A509F, 1:500 dilution), rabbit anti-Ep400 antiserum (home-made, generated against a bacterially expressed and purified peptide corresponding to amino acids 507–661 of mouse Ep400 according to accession number NP_083613, validated on control and knockout mouse tissue, 1:1000 dilution), rabbit anti-Myrf antiserum (home-made, validated on control and knockout mouse tissue, 1:1000 dilution) (28), rabbit anti-Olig2 antiserum (Millipore, #AB9610, Lot# 2060464, 1:1000 dilution), rabbit anti-Pdgfra antiserum (Santa Cruz, #sc-338, Lot# E-1210, 1:300 dilution), rabbit anti-Olig1 antiserum (Millipore, #AB15620, Lot#1987029, 1:1000 dilution), rabbit anti-Nfia antiserum (Active Motif, #39329, Lot#14407002, 1:200 dilution), rabbit anti-Iba1 antiserum (Wako, #019-19741, Lot#SAE6921, 1:250 dilution), rabbit anti-cleaved caspase 3 antiserum (Cell Signaling Technology, #9661, Lot#0043, 1:200 dilution), rabbit anti-Ki67 antiserum (Thermo Fisher Scientific, #RM-9106, Lot#9106S906D, 1:500 dilution), rabbit anti-phosphoH3 (Upstate Biotechnology, #06-570, Lot#19046, 1:1000 dilution), rabbit anti-γH2A.X (Santa Cruz Biotechnology, #sc-517558, Lot#D2118, 1:5000 dilution). For anti-Nkx2.2 antibodies, signal intensity was enhanced by using the TSA-Plus Fluorescence system (PerkinElmer). Secondary antibodies were coupled to Cy3 (Dianova, 1:200 dilution), Cy5 (Dianova, 1:200 dilution) or Alexa Fluor 488 (Molecular Probes, 1:500 dilution) fluorescent dyes. Nuclei were counterstained with DAPI. Some of the antibodies were also used for immunocytochemistry on cells cultured on cover slips and treated with 4% paraformaldehyde for 15 min. Incorporated EdU was visualized using the Click-IT EdU Alexa Fluor 488 Imaging Kit (Thermo Fischer, #C10337). TUNEL was performed according to the manufacturer`s protocol (Chemicon). To combine immunohistochemical staining and *in situ* hybridization, DIG-labeled antisense riboprobes were detected by anti-DIG coupled to DyLight488 (Vector Laboratories, #DI-7488, Lot#ZD0418). Stainings were documented with a Leica DMI6000 B inverted microscope (Leica) equipped with a DFC 360FX camera (Leica).

Electron microscopy

Spinal cord tissue of control and genetically altered mice underwent fixation in cacodylate-buffered fixative containing 2.5% paraformaldehyde and 2.5% glutaraldehyde at P21, P32 and P60. After post-fixation in cacodylate-buffered 1% osmium ferrocyanide, dehydration, embedding in Epon resin, and staining with uranyl acetate and lead citrate, 50 nm sections were examined with a Zeiss Libra electron microscope (Carl Zeiss, Inc.). From these sections, the total number of axons, the number of myelinated axons bigger than 1 μm and the g ratio of myelinated axons were determined.

RNA-Seq and bioinformatic analysis

Total RNA was prepared from FACS-purified oligodendroglial cells obtained at P6 from control and $Ep400^{fl/fl}$ mice additionally carrying $Cnp1^{Cre}$ and $Rosa26^{stopflox\,YFP}$ alleles using the RNeasy Micro Kit (Qiagen). RNA samples were treated with DNase I to remove contaminating DNA. Quality and purity of samples were evaluated using an Agilent 2100 Bioanalyzer (Agilent Technologies Germany). 100 ng were used for library preparation (Ilumina Stranded mRNA Kit). Approximately 80 million reads were generated per library using an Illumina Hiseq 2500 platform sequencer (Next Generation Sequencing Core Facility, FAU Erlangen-Nürnberg) and mapped onto mouse genome mm10 using STAR (version 2.5.1.b). Unique mappings were detected using HTSeq count based on ENSEMBL Genes Version 85. Statistical analysis was carried out using DESeq2 R Version 1.10.1. Gene expression values are deposited in GEO under accession number GSE119127.

Gene ontology (GO) analysis of genes up- and down-regulated in oligodendroglial cells of the *Ep400ΔC* spinal cord at P6 was performed using the Gene Ontology enrichment, analysis and visualization tool (http://cbl-gorilla.cs.technion.ac.il/). Each list of genes was submitted to the Enrichment Analysis Tool for biological processes. For comparison of genes with altered expression in Ep400-deficient oligodendroglial cells to direct target genes of Olig2 and Sox10 or genes with altered expression after loss of Brg1 or Chd7, pairs of gene lists were submitted to the Venn webtool on the BEG homepage (http://bioinformatics.psb.ugent.be/webtools/Venn/). Olig2 target genes were defined as genes associated with Olig2 ChIP-Seq peaks in rat OPCs, immature OL and mature OL (GSE42447, Yu *et al.* 2013 Suppl. Data Set 03), Sox10 target genes as genes associated with ChIP-Seq peaks in rat spinal cord (GSE64703, Lopez-Anido et al. 2015 Supplementary Table S7). To obtain lists of genes deregulated after loss of Brg1 (GSE42443) or Chd7 (GSE72726), respective fastq files were submitted to HTSeq count and statistical analysis was carried out using DESeq2 R Version 1.18.1.

Plasmids and retroviruses

Expression plasmids for parts of Ep400 and Sox10 (see Figure 8B and C) were based on pCMV5 for expression in eukaryotic cells and pGEX-KG for expression in bacteria. Eukaryotic expression plasmids for Ep400 contained mouse sequences (accession number NM_029337). Ep400 fragments (Figure 8C) carried an N-terminal myc-tag, whereas Sox10 fragments (Figure 8B) were C-terminally fused to GST. Sox10 expres-

sion plasmids have been described before (30,31). Expression plasmids for shRNAs were based on pSuper-Neo-GFP and contained the Ep400-specific shRNA (5′-CATCAAGTGGTGGTCACTTTGTATT-3′) or a scrambled version thereof. Luciferase reporter plasmids containing the ECR9 enhancer (*Myrf* ECR9) or the promoter (*Myrf* prom) of the *Myrf* gene were as described (28).

Retroviruses were based on pCAG–IRES–GFP (32) in which GFP was exchanged for tdTomato sequences, and expressed only tdTomato as a marker of transduced cells or tdTomato and Myrf after insertion of the corresponding coding sequence.

Cell culture assays

Rat 33B oligodendroglioma cells (obtained from ECACC #85081901) and human embryonic kidney 293 cells (obtained from ATCC, #CRL-1573) were grown in DMEM supplemented with 10% fetal calf serum (FCS). Rat 33B cells were authenticated by PCR to establish their oligodendroglial identity, but not checked for mycoplasma contamination. They were transfected with polyethylenimine and used for luciferase assays (28). 293 cells were neither authenticated nor checked for mycoplasma contamination because they were only used for preparation of protein extracts after transfection with polyethylenimine (30).

Luciferase assays and protein interaction studies

For luciferase assays in 33B cells, 0.5 μg of pSuper-Neo-GFP-based expression plasmid and 0.5 μg of luciferase reporter were used per 3.5 cm plate. Overall amounts of plasmid in a particular experiment were kept constant by adding empty pSuper-Neo-GFP where necessary. Whole cell extracts were prepared 72 h post transfection by lysing cells in 88 mM MES pH 7.8, 88 mM Tris pH 7.8, 12.5 mM MgOAc, 2.5 mM ATP, 1 mM DTT and 0.1% Triton X-100. Luciferase activities were determined in the presence of 0.5 mM luciferin in 5 mM $KHPO_4$ pH 7.8 by detection of chemiluminescence.

For protein interaction studies, whole cell extracts were prepared by lysing cells in 10 mM HEPES pH 7.9, 10 mM KCl, 0.1 mM EDTA, 0.1 mM EGTA. After addition of NP-40 to 1% final concentration and NaCl to 400 mM, 15 min rotation at 4 °C and 5 min centrifugation, glycerol was added to the supernatant at a final concentration of 10% (31).

Whole cell extracts from primary oligodendroglial cells underwent co-immunoprecipitation with rabbit anti-Sox10 antiserum (home-made, validated on extracts from control and knockout brain tissue) (33) and protein A sepharose beads (GE Healthcare). For GST-pulldown assays, whole cell extracts of transfected 293 cells were incubated with bacterially expressed and purified GST or GST-Sox10 fusion proteins bound to glutathione sepharose beads (31). After extensive washing, bead-bound material was released by boiling in 150 mM Tris–HCl, 6% SDS, 15% β-mercaptoethanol, 30% glycerine, 0,3% bromophenol blue and analyzed after size separation on 10% SDS-polyacrylamide gels by Western blotting. The following primary antibodies and detection reagents were used: rabbit anti-Sox10 antiserum (home-made, 1:1000 dilution), rabbit anti-Ep400 antiserum (home-made, 1:1000 dilution), mouse anti-myc (Cell Signaling, #2276, Lot#0024, 1:10 000 dilution), preimmune serum and horseradish peroxidase coupled to protein A (Zymed, #10-1023, Lot#20873065, 1:3000 dilution). Detection was by chemiluminescence using ECL reagent. Images of Western blots have been cropped for presentation.

Chromatin immunoprecipitation

Chromatin was prepared from cultured rat OPCs, five days differentiated OLs or mouse spinal cord tissue treated with 1% paraformaldehyde and sheared to fragments of ∼200–400 bp in a Bioruptor (Diagenode) (31). After preclearing, chromatin was incubated with rabbit antiserum against Ep400, rabbit antiserum against H2A.Z (Abcam, ab4174, Lot#GR292900-1) or rabbit IgG antibody (Sigma Aldrich, #PP64, Lot#070M768V) before addition of protein A sepharose beads and precipitation. Crosslinks in precipitated chromatin were reversed and DNA was purified by proteinase K treatment, phenol/chloroform extraction and ethanol precipitation. Detection and quantification of specific genomic regions in precipitated DNA was by qPCR on a Bio-Rad CFX96 thermocycler with each reaction performed in triplicates. The ΔΔCt method was used to calculate the percent recovery of a given DNA segment relative to the total input. For ChIP on oligodendroglial cells, the highest relative recovery rate in a particular experiment was set to 1 and all other values were normalized to it. For ChIP on spinal cord tissue, recovery rates were first used to calculate the relative enrichment of anti-Ep400 or anti-H2A.Z antibody over IgG precipitated chromatin, before the highest relative enrichment was again set to 1 and used to normalize all other enrichment rates.

The following DNA regions from the *Myrf* genomic locus were detected by previously published primers (28): dagla (positions −9415 to −9602 in rat and −9392 to −9581 in mouse), fl5 (positions −3973 to −4152 in rat and −2682 to −2891 in mouse), myrf (positions −481 to - 654 in rat and −149 to −364 in mouse), ECR9 (positions +7969 to +8136 in rat and +7586 to +8025 in mouse), ECR11/12 (positions +10463 to +10666 in rat and +10677 to +10885 in mouse) and fl3 (positions +35839 to +36087 in rat and +32539 to +32737 in mouse). Additionally, 5′-GCAGCTCCCTGCTGCCCGAG-3′ and 5′-GACAGTCCCGGCTGGGCTCC-3′ were used to amplify positions −86 to −253 in rat, 5′-GTACTTAGCACAGAGTATCC 3′ and 5′-CACAGACTTTAAGGCAAGGC-3′ to amplify −149 to −316 in mouse (–TS), 5′-CCAGCCAACCCCGC GGTCTC-3′ and 5′-CTCGAAGCCATTCATCTCGC-3′ to amplify +71 to +225 in rat and 5′-GCGATCAACCTT CTGCTCTG-3′ and 5′-CTCGAAGCCATTCATCTCGC-3′ to amplify +40 to +214 in mouse (+TS).

Quantifications and statistical analysis

Results from independent specimens or experiments were treated as biological replicates. Sample size was $n \geq 3$ for all molecular biology experiments and experiments using cell cultures or mice as common for this kind of study. No data

were excluded from the analysis. Randomization was not possible. GraphPad Prism6 (GraphPad software, La Jolla, CA, USA) was used to determine whether differences in cell numbers, luciferase activities or immunoprecipitated DNA were statistically significant by two-tailed Student's t tests ($^{*}P \leq 0.05$; $^{**}P \leq 0.01$, $^{***}P \leq 0.001$). Variance between statistically compared groups was similar.

RESULTS

Ep400 is broadly expressed in the developing CNS

To analyze Ep400 occurrence in the CNS by immunohistochemistry, we first generated an antiserum directed against an epitope corresponding to amino acids 507–661 of the mouse protein. Immunohistochemical staining of sections of the early postnatal spinal cord revealed Ep400 expression in virtually all nuclei. This included cells positive for the pan-neuronal marker NeuN, the astroglial markers Nfia and Gfap, the microglial marker Iba1, and the oligodendroglial markers Sox10 and Olig2 (Figure 1A–F). Among cells of the oligodendroglial lineage Ep400 was found in Pdgfra-positive OPCs, Nkx2.2-positive immature OLs and Mbp-positive myelinating OLs (Figure 1G–I).

Even during early embryonic development, Ep400 was already expressed in almost all nuclei of the spinal cord, including those of neuroepithelial precursor cells in the ventricular zone (Figure 1J, L and N). Mice with a *Nestin::Cre*-mediated Ep400 deletion (*Ep400ΔN*) lacked almost all of the immunohistochemical Ep400 signal throughout the early CNS (Figure 1K, M and O), proving the specificity of the antiserum. We conclude that Ep400 is expressed in all cell types of the early rodent CNS. In the oligodendroglial lineage, Ep400 is present at all stages. This is in line with previously published RNA-Seq data for *Ep400* transcripts (34).

Ep400 is not required for OL specification or prenatal development

For a systematic investigation of the role of Ep400 in OL development, we concentrated on the mouse spinal cord as a well-characterized model region. The use of *Nestin::Cre* allows gene inactivation before OPCs are specified from the pMN domain in the ventral part of the ventricular zone (33). When spinal cord sections of *Ep400ΔN* mice were analyzed shortly after the onset of OPC specification at embryonic day (E) 12.5 by immunohistochemistry, no obvious alterations in position and number of Olig2-positive pMN precursor cells or Sox10-positive OPCs were apparent relative to the control (Figure 1P, Q, T, U and X) despite efficient Ep400 deletion (Figure 1K, M and O). OPC number and distribution were still comparable on spinal cord sections of *Ep400ΔN* embryos and control littermates at E14.5 (Figure 1R, S, V, W and Y) arguing that Ep400 is not required for OPC specification or early lineage progression.

To focus on the cell-autonomous effects of Ep400 on embryonic OL development after the specification process, we exchanged the *Nestin::Cre* for a *Sox10::Cre* allele. In the CNS of the resulting *Ep400ΔS* mice, Ep400 deletion is restricted to the OL lineage (Supplementary Figure S1A–F). As previously documented for other genes (35), *Sox10::Cre*-dependent Ep400 deletion is furthermore very efficient reaching 46% at E12.5 and 90% at E14.5 in spinal cord oligodendroglia (Supplementary Figure S1G). However, there is also widespread Ep400 deletion outside the CNS in several neural crest derivatives (21). As a consequence, *Ep400ΔS* embryos exhibit severe neural crest-related defects including orofacial clefting and die at birth.

As already observed in *Ep400ΔN* embryos, OPCs are present in normal numbers and regular distribution throughout the mutant spinal cord of *Ep400ΔS* embryos at E12.5 and at E14.5 (Supplementary Figure S1H–Q). We were still unable to detect differences in the number of oligodendroglial cells at E18.5 as judged by immunohistochemistry for the OL lineage marker Olig2 (Figure 2A–C). At this time, most oligodendroglial cells in the spinal cord represent OPCs. According to immunohistochemical Pdgfra detection, OPC numbers were unchanged (Figure 2D–F). However, oligodendroglial cells that had started terminal differentiation and initiated myelin gene expression were drastically reduced as obvious from immunohistochemistry with anti-Myrf and anti-Mbp antibodies (Figure 2G–L). This was confirmed by *in situ* hybridization with *Mbp*- and *Plp1*-specific probes (Figure 2M–R). Immunohistochemical stainings for proliferation (Ki67) and apoptosis (cleaved caspase 3) markers yielded similar results in *Ep400ΔS* embryos and control littermates (Figure 2S and T). We conclude that oligodendroglial development proceeds without major disturbances during embryogenesis until alterations become apparent at the onset of terminal differentiation around the time of birth.

Ep400 is required postnatally for OL survival

As *Ep400ΔS* mice do not allow to follow OL differentiation postnatally, we switched to the $Cnp1^{Cre}$ allele for conditional *Ep400* deletion. $Cnp1^{Cre}$-dependent deletion in the CNS is also restricted to the oligodendroglial lineage (Supplementary Figure S1R–W) but delayed relative to *Sox10::Cre*-dependent deletion as it occurs only in late OPCs. Nevertheless, deletion rates in the oligodendroglial lineage were already above 80% at postnatal day 1 (P1) and stayed at this value until P60 (Supplementary Figure S1X). $Cnp1^{Cre}$ is also active outside the CNS but has a more restricted occurrence than *Sox10::Cre*. The resulting *Ep400ΔC* mice were born alive at normal Mendelian ratios, but after one month, the first *Ep400ΔC* mice died (Figure 3A). The median survival was 44 days. By 2 months of age, survival rates were down to 35% and only 2% survived the third month. *Ep400ΔC* mice shivered, exhibited an unsteady gait and showed signs of ataxia as expected for a central hypo- or dysmyelination phenotype.

At P1, *Ep400ΔC* mice reproduced the phenotype observed shortly before birth in *Ep400ΔS* mice. The number of spinal cord oligodendroglial cells as defined by the expression of Olig2, Sox10 or Olig1 was comparable to the control (Figure 3B–D). Pdgfra-positive OPCs were also present at normal numbers at P1 in *Ep400ΔC* mice and there were no alterations in the number of Ki67-positive cells relative to the control (Figure 3E and F). In contrast, the numbers of Nkx2.2- or Myrf-positive immature OLs were dramatically reduced at this stage, as was the number of Plp1-expressing

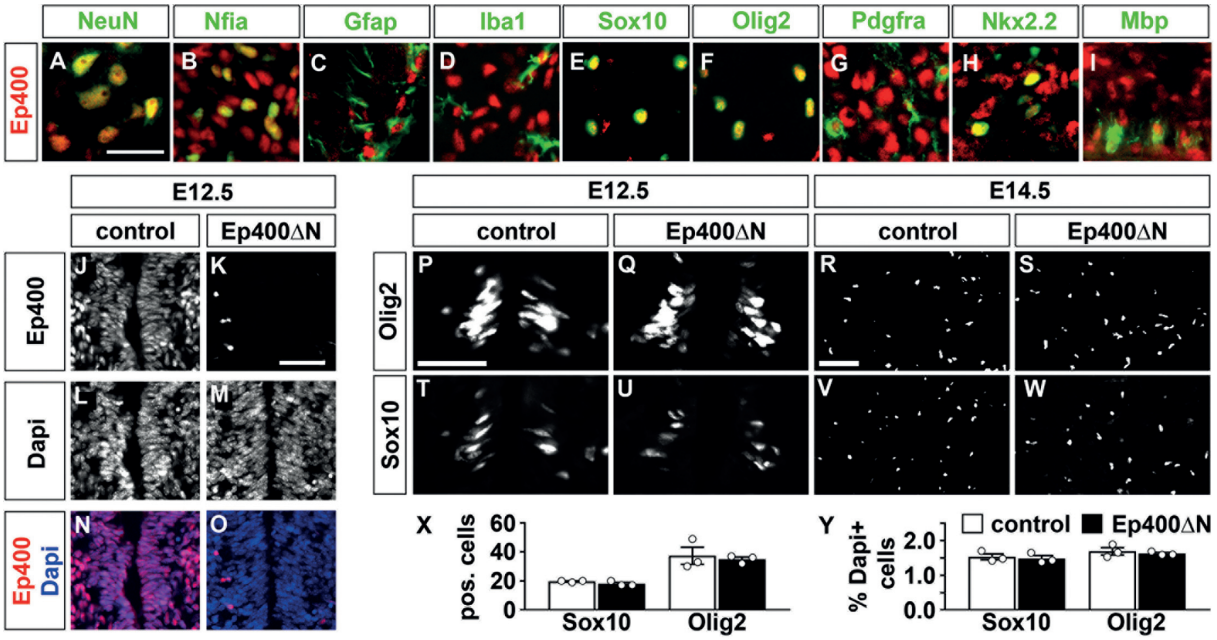

Figure 1. Ep400 occurrence in the mouse spinal cord and dispensability for OPC specification. (**A–I**) Localization of Ep400 (red) determined by co-immunohistochemistry on spinal cord tissue at postnatal day 1 (P1) with the following CNS cell type markers (green): NeuN (A), Nfia (B), Gfap (C), Iba1 (D), Sox10 (E), Olig2 (F), Pdgfra (G), Nkx2.2 (H), Mbp (I). (**J–O**) Ep400 deletion in *Ep400*$^{fl/fl}$ *Nestin::Cre* (*Ep400ΔN*, K,M,O) embryos as determined by Ep400 immunohistochemistry (J,K,N,O) at E12.5 relative to age-matched controls (J,L,N). Nuclei were counterstained with Dapi (L–O). Shown is the ventral spinal cord surrounding the ventricular zone (**P–W**) Immunohistochemistry with antibodies directed against Olig2 (P–S) and Sox10 (T–W) on transverse spinal cord sections of control and *Ep400ΔN* embryos at E12.5 (P,Q,T,U) and E14.5 (R,S,V,W). Shown is the region around the pMN domain (P, Q, T, U) and ventral mantle zone (R,S,V,W). Scale bars: 30 μm (A) and 50 μm (K, P, R). (**X**, **Y**) Quantifications of Olig2 and Sox10 positive cells in spinal cord of control and *Ep400ΔN* embryos at E12.5 (X) and E14.5 (Y) ($n = 3$ embryos per genotype, counting three separate sections each). Mean absolute cell numbers per section (X) or relative numbers normalized to DAPI (Y) ± SEM are presented. No statistically significant difference between the genotypes was detected.

cells as a readout for myelinating OLs (Figure 4A, B and D).

When the number of oligodendroglial cells was followed in the spinal cord of *Ep400ΔC* mice during the first two months, reductions relative to the control became evident at P6 for most markers and reached statistical significance for all at P14 (Figure 3B–D, G–N and Supplementary Figure S2A–P). By this time, there were approx. 40% less oligodendroglial cells present in the spinal cord of *Ep400ΔC* mice. This difference persisted throughout the following six weeks. Pdgfra-positive OPCs were not proportionately affected by this loss of oligodendroglial cells. Their number was comparable to the control until P32 (Figure 3E, O–Q and S–U). Before and at P14, there were furthermore no differences in the number of Ki67-positive, phospho-H3-positive cells or in the EdU-incorporation rates (Figure 3F and Supplementary Figure S2Q and R) indicating that the reduced number of oligodendroglial cells is not caused by depletion of the OPC pool or a decrease in their proliferative capacity. At P60, numbers of Pdgfra- and Ki67-positive cells were even increased (Figure 3E, F, R and V) as if remaining OPCs tried to compensate for the decrease of oligodendroglial cells by enhanced proliferation.

To investigate whether oligodendroglial cells were lost by apoptosis, we performed immunohistochemical stainings against cleaved caspase 3 (Figure 3W). The number of oligodendroglial cells with cleaved caspase 3 was indeed elevated from P6 onwards. Increased rates of apoptosis were also confirmed by TUNEL at all analyzed time points (Figure 3X). These studies show that oligodendroglial cells in *Ep400ΔC* mice are compromised in their survival. They furthermore point to a role of Ep400 in cell survival during late oligodendroglial development as increased cell death starts to show one week after birth and largely affects OLs.

Ep400 is required for terminal differentiation of OLs

Terminal differentiation defects are already visible before birth in the spinal cord of *Ep400ΔS* mice and immediately after birth in *Ep400ΔC* mice, when survival of oligodendroglial cells is still normal. It follows that impaired differentiation is not a simple consequence of compromised survival. When OL differentiation was analyzed during the first two months, we noticed a strong decrease of all OL markers including Nkx2.2, Myrf, CC1, Plp1 and Mbp (Figure 4A–T and Supplementary Figure S3A–P). Despite minor variations, substantial differences were visible for all markers at most time points arguing that the differentiation defect persists in *Ep400ΔC* mice. In fact, the impact of Ep400 on OL differentiation is probably bigger than judged from marker analysis, as OLs that escaped recombination contributed to OL marker gene expression. By combining *Plp1 in situ* hybridization with Ep400 immunohistochemistry, we found both Ep400-positive and Ep400-negative OLs that expressed *Plp1* (Supplementary Figure S3Q). Interestingly, the myelination defect did not increase number or activa-

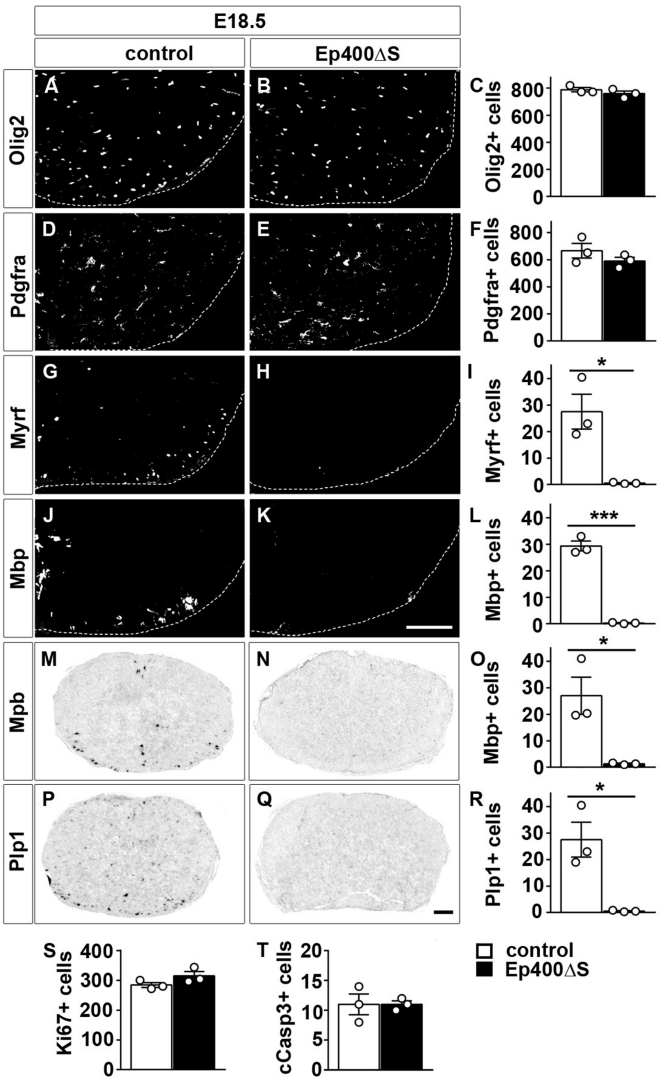

Figure 2. Normal prenatal OPC development and impaired induction of oligodendroglial differentiation in the absence of Ep400. (**A–T**) Analysis of oligodendroglial marker expression by immunohistochemistry (A, B, D, E, G, H, J, K) and *in situ* hybridization (M, N, P, Q) on transverse spinal cord sections of control (A, D, G, J, M, P) and *Ep400ΔS* (B, E, H, K, N, Q) embryos at E18.5. Antibodies were directed against Olig2 (A, B), Pdgfra (D, E), Myrf (G, H), and Mbp (J, K). Riboprobes recognized *Mbp* (M, N) and *Plp1* (P, Q) mRNA. Scale bars, 100 μm (K) and 200 μm (Q). From these and similar stainings for Ki67 (S) and cleaved caspase 3 (cCasp3, T) quantifications were performed for control (white bars) and *Ep400ΔS* (black bars) spinal cord (n = 3 embryos per genotype, counting three separate sections each). Mean cell numbers ± SEM per section are presented. Statistical significance was determined by two-tailed Student's *t*-test ($^{*}P \leq 0.05$; $^{***}P \leq 0.001$).

tion status of microglia as judged by Iba1 stainings (Supplementary Figure S3R) but went along with an increased astrogliosis as evident from higher Gfap immunoreactivity (Supplementary Figure S3S–V).

As OL differentiation defects usually go along with myelination problems, we also performed ultrastructural analyses on spinal cord tissue at P21, P32 and P60. Electron microscopy revealed that the percentage of myelinated axons with a calibre ≥ 1 μm is strongly reduced in *Ep400ΔC* mice at all times analyzed (Figure 5A, D and E, Supplementary Figure S4B, C, E and F). At P60, the effect was even more dramatic than at the earlier time points (Figure 5A). This may suggest that myelin loss is progressive. Additionally, those axons that remained myelinated in *Ep400ΔC* mice had thinner myelin sheaths (Figure 5C, D and E, Supplementary Figure S4A–F) and exhibited significantly increased g ratios (Figure 5B). Both small and large calibre axons appear similarly affected (Figure 5C, Supplementary Figure S4A and D). Additionally, there were obvious abnormalities in the myelin of *Ep400ΔC* mice (Figure 5E and F, Supplementary Figure S4C and F). These included myelin outfoldings, myelin sheaths that are not completely closed around axons, and myelin sheaths around multiple, sometimes already myelinated axons. There were also few smaller axons that exhibited hypermyelination (Figure 5F, right panel). Despite persistent hypomyelination and continuous occurrence of myelin abnormalities, axon numbers were comparable to controls at P60 arguing against a substantial axonal degeneration in *Ep400ΔC* mice (Supplementary Figure S4G).

While our studies focused on the spinal cord, we also analyzed oligodendroglial marker gene expression in the forebrain at P32 (Supplementary Figure S5A–N). These studies confirmed the oligodendroglial differentiation and OL survival defect in both corpus callosum and cortex as representative white and grey matter regions.

Ep400 deletion changes the oligodendroglial expression profile

Using FACS we purified oligodendroglial cells from acutely dissociated brain of *Ep400ΔC* pups that additionally contained a *Rosa26*$^{stopflox YFP}$ reporter. *Rosa26*$^{+/stopflox YFP}$ *Cnp1*$^{+/Cre}$ mice served as control. We chose to purify at P6 because oligodendroglial cells can be obtained rapidly after gentle CNS tissue dissociation thus minimizing preparation-induced changes of expression. Additionally, we wanted to study the expression profile at an early time point to avoid secondary changes of gene expression in mutant oligodendroglial cells. Principal component analysis confirmed clustering of replicate samples from control and *Ep400ΔC* mice (Figure 6A). As evident from the MA plot most genes were comparably expressed in oligodendroglial cells from both genotypes (Figure 6B). Expression was ≥2-fold increased for 672 genes in oligodendroglial cells from *Ep400ΔC* mice, and ≥2-fold decreased for 359 genes (Figure 6C). When the 5000 most up- or downregulated genes in *Ep400ΔC* mice were compared to Olig2 or Sox10 target genes previously determined by ChIP-Seq we found some overlap (Figure 6D and E). Additionally, a fraction of genes was similarly dysregulated in *Ep400ΔC* mice as in mice with oligodendroglial *Brg1* or *Chd7* inactivation (Figure 6F and G). However, none of the analyses pointed to an especially tight and preferential relationship of Ep400 with any of the analyzed epigenetic or transcriptional regulators on a global scale. In line with such a conclusion, *Ep400ΔC* mice with an additional loss of one *Brg1* allele exhibited comparable oligodendroglial differentiation and survival defects as *Ep400ΔC* mice (Supplementary Figure S6A–N).

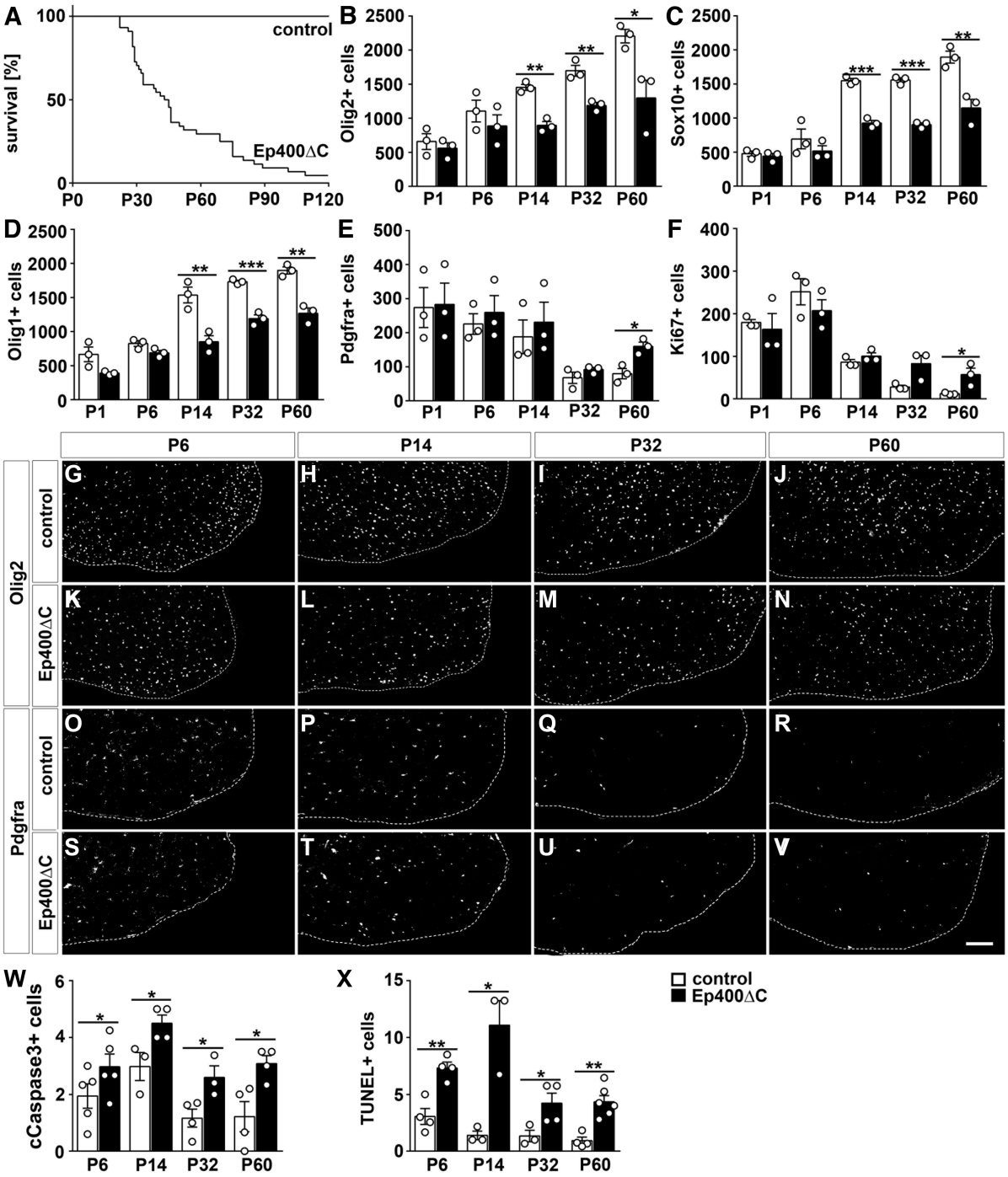

Figure 3. Reduced postnatal survival of oligodendroglial cells in the absence of Ep400. (**A**) Survival curve of control and *Ep400*$^{fl/fl}$ *Cnp1*$^{+/Cre}$ (*Ep400ΔC*) mice during the first 4 months of life. (**B–F**) Quantifications of Olig2- (B), Sox10- (C), Olig1- (D), Pdgfra- (E) and Ki67- (F) positive oligodendroglial cells in spinal cord of control (white bars) and *Ep400ΔC* (black bars) mice at P1, P6, P14, P32 and P60 (n = 3 mice per genotype, counting three separate sections each). Mean cell numbers ± SEM per section are presented. (**G–V**) Representative immunohistochemical stainings of spinal cord sections from control (G–J, O–R) and *Ep400ΔC* (K–N, S–V) mice from P6 to P60 with antibodies directed Olig2 (G–N) and Pdgfra (O–V). Shown is the right ventral horn, placed on a black background. Scale bar: 100 μm. (**W**, **X**) Quantifications of cleaved caspase 3- (cCasp3, W), and TUNEL- (X) positive oligodendroglial cells in spinal cord of control (white bars) and *Ep400ΔC* mice (black bars) at P6, P14, P32 and P60 (n = 3–5 mice per genotype, counting three separate sections each; mean values ± SEM). Statistical significance was determined by two-tailed Student's *t*-test ($^{*}P \leq 0.05$; $^{**}P \leq 0.01$; $^{***}P \leq 0.001$).

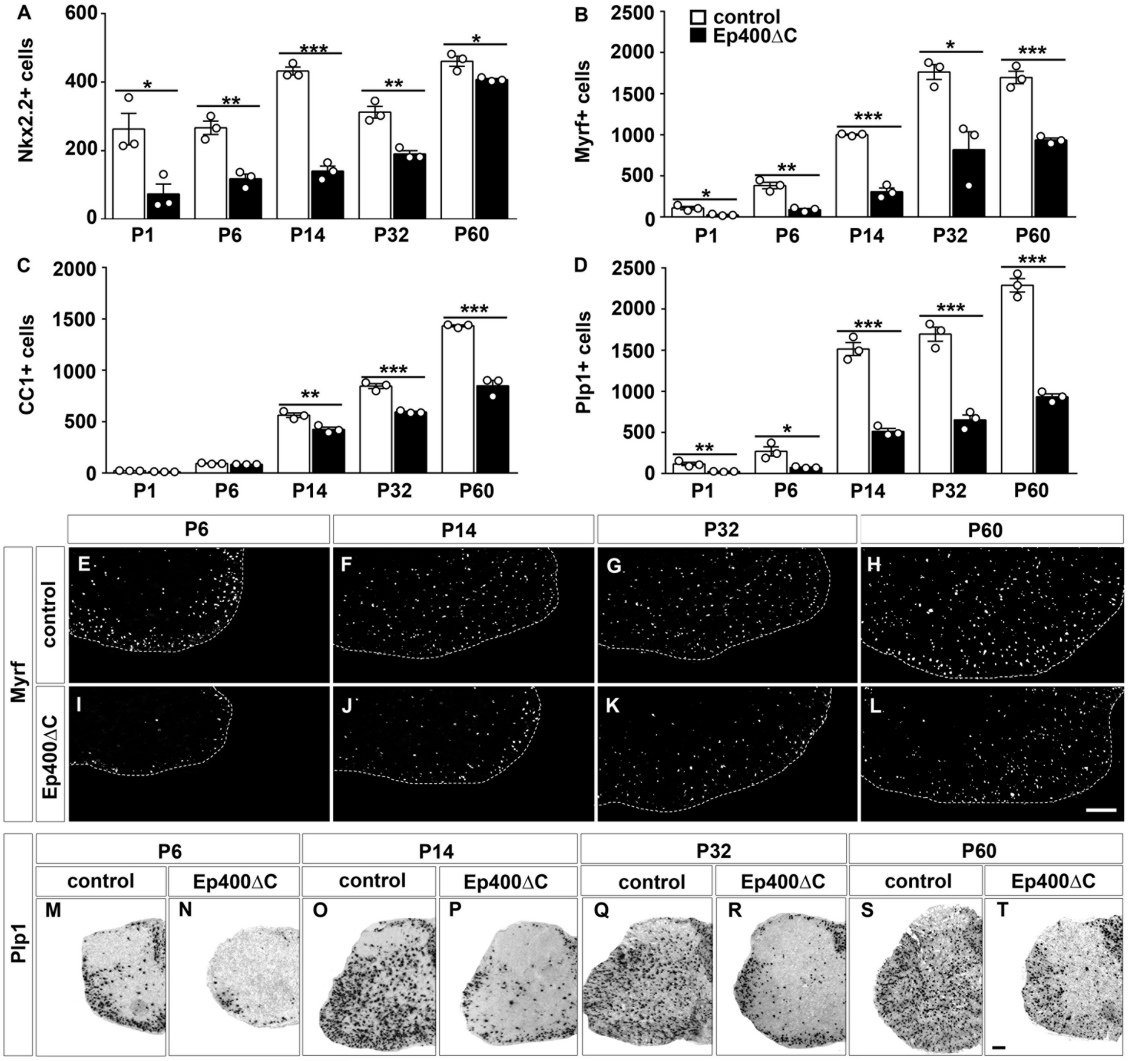

Figure 4. Impaired OL differentiation in the absence of Ep400. (**A–D**) Quantifications of Nkx2.2- (A), Myrf- (B), CC1- (C) and *Plp1*- (D) positive oligodendroglial cells in spinal cord of control (white bars) and *Ep400ΔC* (black bars) mice at P1, P6, P14, P32 and P60 (n = 3 mice per genotype, counting three separate sections each). Mean cell numbers ± SEM per section are presented. (**E–T**) Representative immunohistochemical stainings with antibodies directed Myrf (E–L) and *in situ* hybridizations with a *Plp1*-specific antisense riboprobe (M–T) of spinal cord sections from control (E–H, M, O, Q, S) and *Ep400ΔC* (I–L, N, P, R, T) mice from P6 to P60. Shown is the right ventral horn placed on a black (E–L) or left half of spinal cord on a white (M–T) background. Scale bar: 100 μm (L,T). Statistical significance was determined by two-tailed Student's *t*-test ($^{*}P \leq 0.05$; $^{**}P \leq 0.01$; $^{***}P \leq 0.001$).

GO analysis of downregulated genes in oligodendroglial cells of *Ep400ΔC* mice revealed an enrichment of the terms 'response to amino acid stimulus', 'myelination', 'axon ensheathment' and 'neuron ensheathment' as well as 'collagen fibril organization' among biological processes (Figure 6H). In a panel of OL-enriched genes selected according to literature and published RNA-Seq data (34), the vast majority exhibited downregulation in oligodendroglial cells of *Ep400ΔC* mice (Figure 6I). This did not only concern terminal differentiation and myelination genes such as *Plp1, Mbp, Mog* and *Nfasc*, but also regulators of the process such as *Sox10*, *Nkx2.2*, *Olig2, Olig1*, *Myrf* and *Fyn* arguing that Ep400 may influence expression of differentiation and myelination directly or indirectly by influencing the activity of key transcriptional network components.

When upregulated genes underwent a comparable analysis the GO terms 'regulation of Tnf secretion', 'nucleic acid metabolism', protein ubiquitination', 'small protein conjugation to proteins', 'response to DNA damage' and 'double-strand break repair' were enriched (Figure 6J). Considering that ubiquitination has an established role in DNA repair (36) and that Ep400 activity had previously been associated with DNA damage and damage repair (16), we also analyzed a set of genes linked to this process and found most of them upregulated (Figure 6K). This is intriguing as it may indicate that altered response to DNA damage in oligodendroglial cells of *Ep400ΔC* mice may be responsible for the decreased survival. In line with such an assumption, many more cells were positive for the DNA damage marker γH2A.X in primary oligodendroglial cell cultures from *Ep400ΔC* than from control mice (Figure 6L–P), and these γH2A.X-positive cells outnumbered the cells labeled by cleaved caspase 3 arguing that increased DNA damage

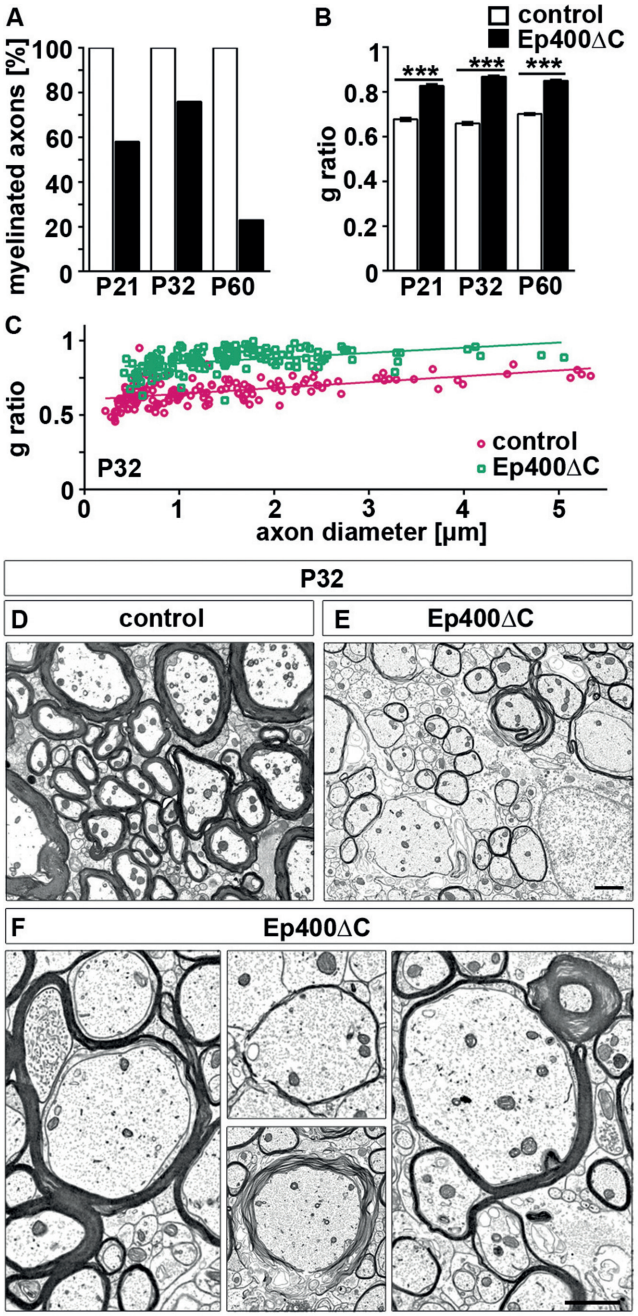

Figure 5. Altered myelin ultrastructure in the spinal cord of *Ep400ΔC* mice. (**A**, **B**) Quantification of the number of myelinated axons as percent of total axons with a diameter ≥1 μm (A) and the mean g ratio (B) in ultrathin spinal cord sections of control (white bars) and *Ep400ΔC* (black bars) mice at P21, P32 and P60. (**C**) Scatter blot of g ratios for single axons in control (magenta) and *Ep400ΔC* (green) spinal cord at P32. (**D**–**F**) Representative electron microscopic pictures of control and *Ep400ΔC* spinal cord at P32 in overview (D,E) and at higher magnifications (F). Higher magnifications depict various myelin abnormalities. Scale bars: 1 μm. Statistical significance was determined by two-tailed Student's *t*-test ($^{***}P \leq 0.001$).

in Ep400-deficient oligodendroglial cells precedes apoptotic changes (Figure 6Q–U).

Ep400 influences key components of the oligodendroglial gene regulatory network

To check for a direct influence of Ep400 on the oligodendroglial gene regulatory network, we concentrated on the *Myrf* gene (Figure 7A) as the encoded transcription factor is considered to be the master regulator of OL differentiation (37). Induction of *Myrf* in immature OL has previously been shown to depend on Sox10 which directly binds to ECR9, an evolutionary conserved enhancer in the first intron of the gene (28).

By performing chromatin immunoprecipitation (ChIP) on primary cells with antibodies directed against Ep400 and probing several regions in the *Myrf* locus in OPCs and OLs we found Ep400 selectively enriched in the vicinity of the transcriptional start site and on ECR9 (Figure 7B and D). The localization around the transcriptional start site changed slightly upon differentiation. Whereas Ep400 was preferentially localized to the region immediately downstream of the transcriptional start site in OPCs, it was found both on the promoter and downstream of the transcriptional start site in OL. Ep400 is thus present on the *Myrf* gene before its induction in immature OLs. The presence over a broader region around the transcriptional start site in OLs may be indicative of the induction process.

As Ep400 is known to catalyse the exchange of H2A against H2A.Z in chromatin (13,14), we also performed ChIP experiments on the *Myrf* locus with H2A.Z-specific antibodies (Figure 7C and E). H2A.Z occupancy followed Ep400 binding patterns on the promoter. In OPCs, H2A.Z was primarily detected downstream of the transcriptional start site of *Myrf*. In OLs, we found H2A.Z substantially enriched both immediately upstream and downstream of the transcriptional start site relative to control IgG.

When chromatin was prepared from spinal cord of control mice at P6 and used for ChIP, we were able to reproduce Ep400 and H2A.Z enrichment on *Myrf* promoter and ECR9 (Figure 7F and G). This enrichment was strongly reduced when chromatin from spinal cord of age-matched *Ep400ΔC* mice was used (Figure 7F and G). At P6, oligodendroglial cells represent a minor fraction of the spinal cord cell population. Considering that all other cells also express Ep400 but not Myrf, Ep400 occupancy of this gene is specific for oligodendroglial cells.

An ECR9-dependent role of Ep400 in *Myrf* activation is also supported by reporter assays performed in transiently transfected 33B oligodendroglioma cells (Figure 7H). Co-transfection of an Ep400-specific shRNA reduces activity of a luciferase reporter under control of the *Myrf* ECR9 to levels obtained with the *Myrf* minimal promoter.

As ECR9 is bound by Ep400 and by Sox10 (28), we also investigated whether the two proteins physically interact. Co-immunoprecipitation experiments showed that antibodies directed against Sox10 were not only able to precipitate endogenous Sox10 from OL extracts, but also Ep400 (Figure 8A). To confirm the interaction and map the responsible domains, we performed pulldown experiments with bacterially produced and purified fusion pro-

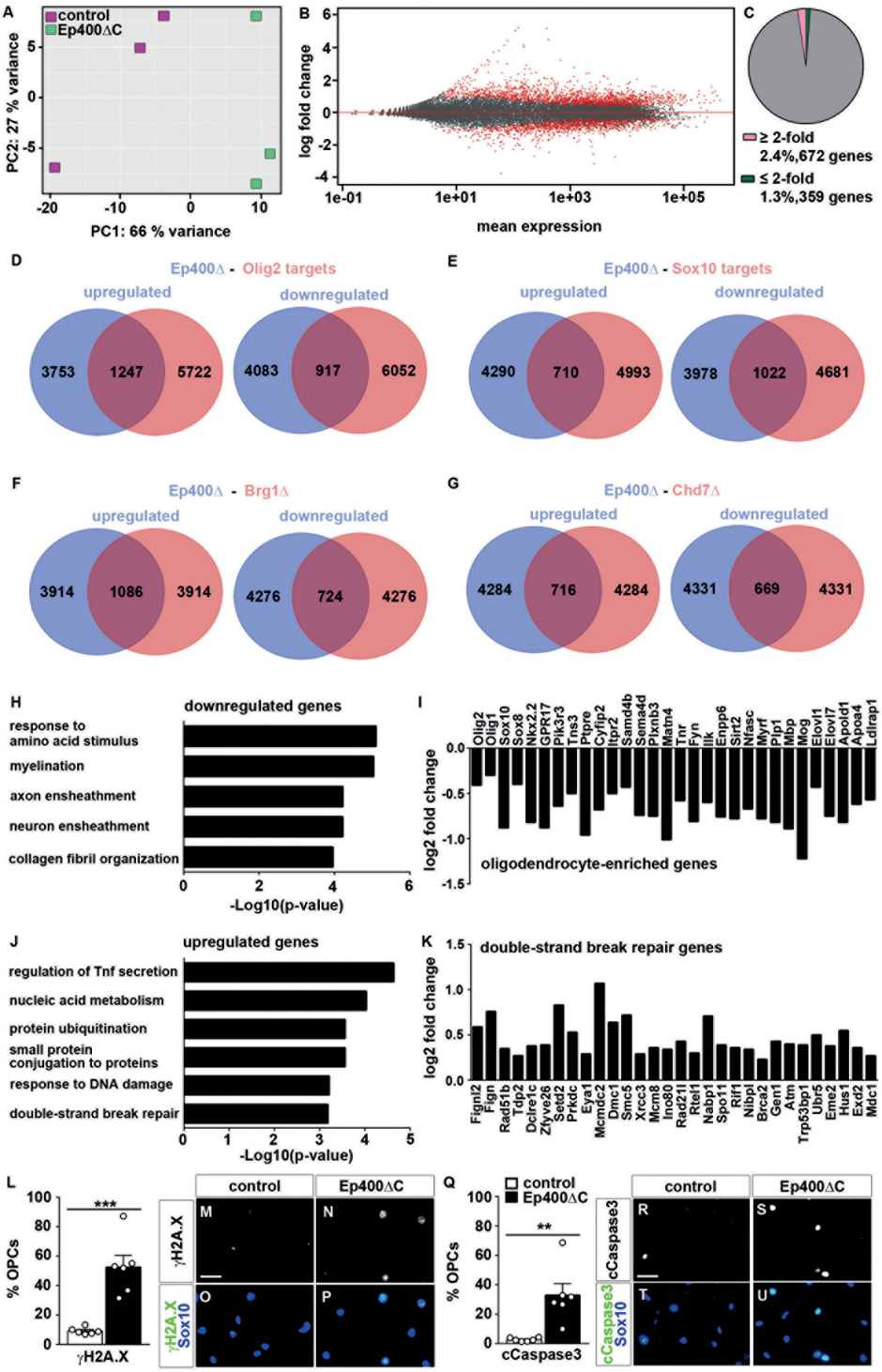

Figure 6. Altered oligodendroglial gene expression in the absence of Ep400. (**A**) Principal component analysis blot of RNA samples from control (magenta) and *Ep400ΔC* (green) primary OL used for RNA-Seq. (**B**) MA plot depicting the overall gene expression changes in *Ep400ΔC* primary OL relative to control primary OL. (**C**) Pie chart depicting the percentage of genes with ≥2-fold increased (pink) and ≤2-fold decreased (dark green) expression ($P \leq 0.05$) in *Ep400ΔC* OL. (**D–G**) Comparison of the 5000 most up- or downregulated genes in *Ep400ΔC* primary OL (blue) with genes having nearby ChIP-Seq peaks (red) for Olig2 (D, acc. to GSE42447), Sox10 (E, acc. to GSE64703), or exhibiting dysregulation after oligodendroglial Brg1 (F, acc. to GSE42443) and Chd7 (G, acc. to GSE72726) deletion. (**H**, **I**) Gene ontology analysis for genes downregulated in primary OL upon Ep400 loss (H), and compilation of those associated with OL differentiation and myelination (I). (**J**, **K**) Gene ontology analysis for genes upregulated in primary OL upon Ep400 loss (J), and compilation of those associated with DNA repair mechanisms (K). (**L–U**) Quantifications of γH2A.X- (L) and cleaved caspase 3-positive (Q) mouse OL from control (white bar) and *Ep400ΔC* (black bar) mice cultured for one day under differentiating conditions using immunocytochemical stainings ($n = 6$ separate cultures per genotype. Presentations are as percentage of Sox10-positive cells; mean values ± SEM). Representative immunocytochemical stainings are shown for γH2A.X (M–P) and cleaved caspase 3 (R–U) (white and green) with OL counterstained by anti-Sox10 antibodies (blue). Scale bar 25 μm (M, R). Statistical significance was determined by two-tailed Student's *t*-test ($^{**}P \leq 0.01$; $^{***}P \leq 0.001$).

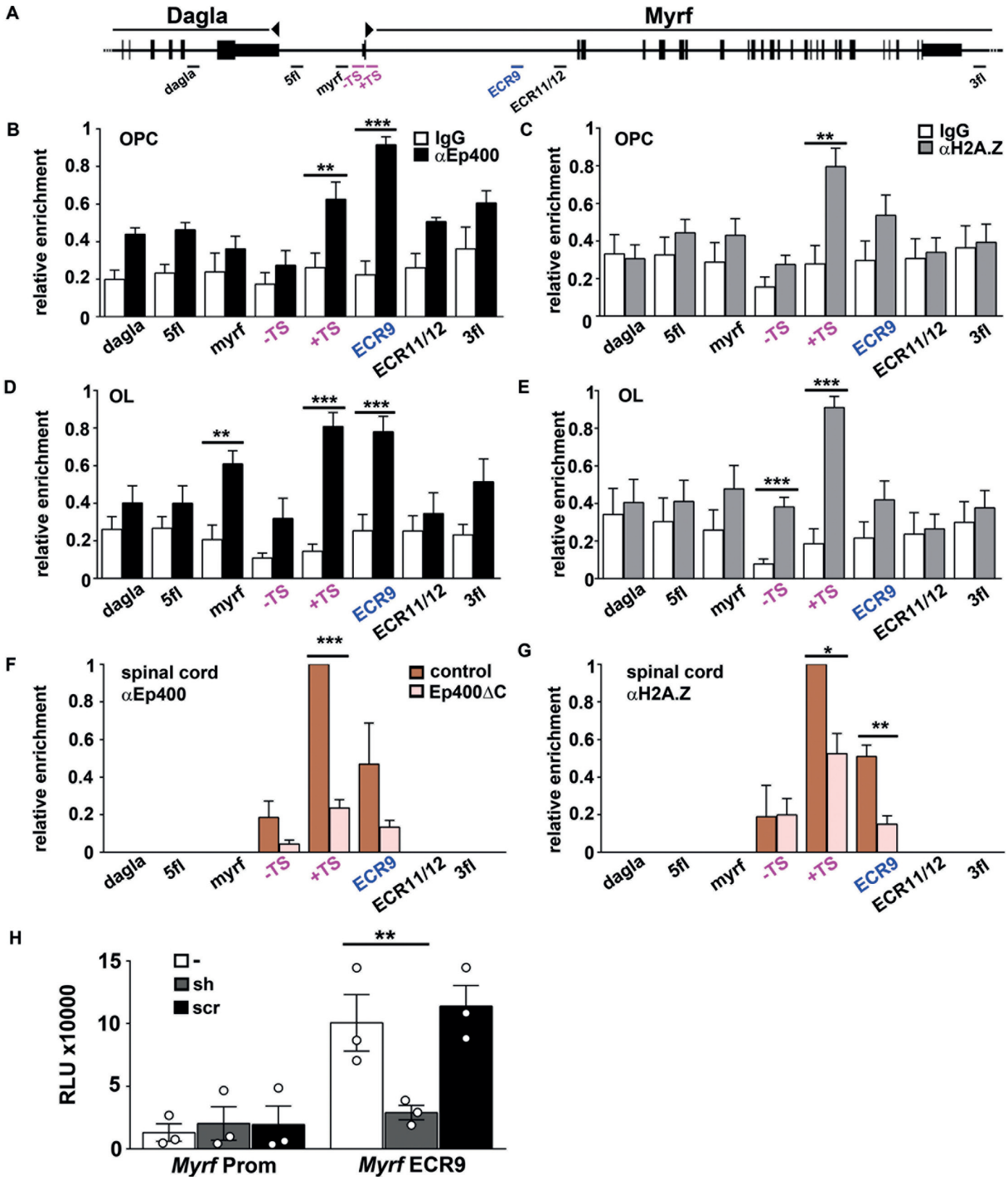

Figure 7. Functional interactions of Ep400 and Sox10 on the *Myrf* gene. (**A**) Schematic representation of the *Myrf* gene in its genomic context (continuous long horizontal line). Exons of *Myrf* and adjacent *Dagla* gene are depicted as vertical bars, regions probed in ChIP (dagla, 5fl, myrf, –TS, +TS, ECR9, ECR11/12, 3fl) as short horizontal lines at the bottom. (**B–G**) ChIP experiments were performed on crosslinked, sheared chromatin of primary rat oligodendroglial cells (B–E) kept under proliferative (B, C) or differentiating (D, E) conditions and mouse spinal cord (F, G). Oligodendroglial cells were prepared from controls (brown bars in F, G) and *Ep400ΔC* (light pink bars in F,G) at P6. Several regions distributed throughout the *Myrf* locus were analyzed by quantitative PCR in input and precipitated chromatin with IgG control (B–E) or antibodies directed against Ep400 (B, D, F) and H2A.Z (C, E, G). Presentations are relative enrichments. Experiments were performed eight (B-E) or three times (F, G) and the highest value of each run was set to one. Results are presented as mean values ± SEM. (**H**) Activity of a luciferase reporter under control of *Myrf* promoter (*Myrf* Prom) or *Myrf* ECR9 in 33B extracts 72 h after transient transfection in the absence (–) or presence of a Ep400-specific shRNA (sh) or a scrambled version (scr). Presentation is in relative light units (RLU) ($n = 3$ transfections, each performed in triplicates; mean values ± SEM).

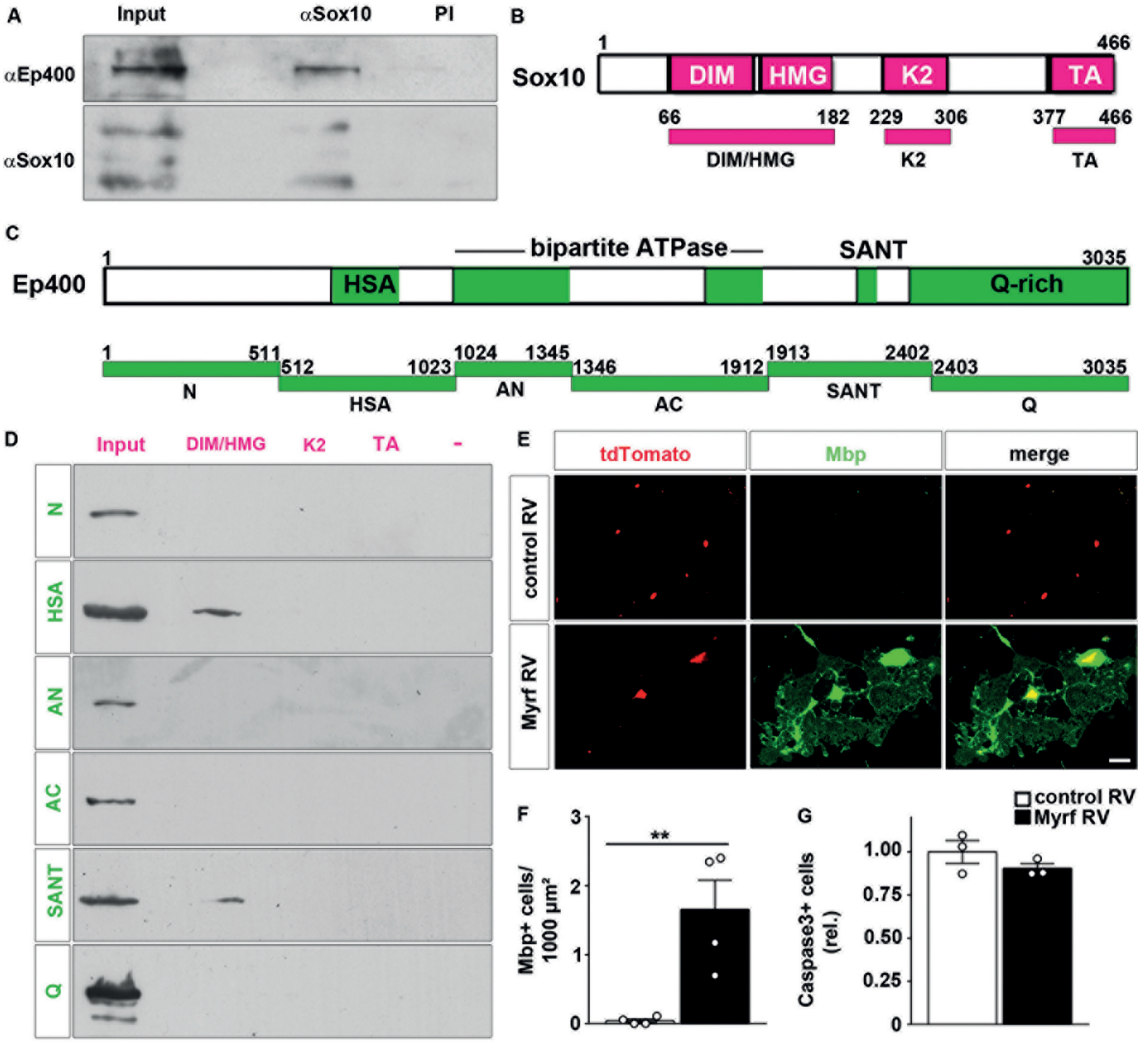

Figure 8. Physical interactions of Ep400 and Sox10 and Myrf-dependent phenotypic rescue of Ep400-deficient OLs. (**A**) Co-immunoprecipitation of Ep400 from rat oligodendroglial cell extracts (input) with antibodies directed against Sox10 (αSox10) or pre-immune serum (PI). The upper Western blot was incubated with antibodies specific for Ep400, the lower with antibodies specific for Sox10. (**B**) Scheme of Sox10, its functional dimerization (DIM), HMG, K2 and transactivation (TA) domains as well as subfragments (DIM/HMG, K2, TA) used in GST-pulldown experiments. Numbers represent amino acid residues at N- or C-terminal positions. (**C**) Scheme of Ep400, its functional HSA, bipartite ATPase, SANT and Q-rich domains as well as subfragments (N, HSA, AN, AC, SANT, Q) used in GST-pulldown experiments. (**D**) GST-pulldown assays with HEK293 extracts containing myc-tagged Ep400 subfragments N, HSA, AN, AC, SANT and Q (input) using bacterially expressed GST (-) or GST fused to Sox10-subfragments DIM/HMG, K2 and TA, bound to glutathione sepharose beads as baits. Bound Ep400 subfragments were visualized by Western blots using antibodies directed against the myc tag. (E,F) Quantification of Mbp-positive mouse OL from *Ep400ΔC* mice transduced with control (control RV) and Myrf-expressing retroviruses (Myrf RV) (both tdTomato-positive) cultured for six days under differentiating conditions following immunocytochemical stainings (n = 4 separate cultures; mean values ± SEM). Representative stainings are shown for tdTomato (red) and Mbp (green). Scale bar 50 µm. (G) Quantification of cleaved caspase3-positive mouse OL from *Ep400ΔC* mice transduced with control and Myrf-expressing retroviruses cultured for one day under differentiating conditions following immunocytochemical stainings ($n = 3$ separate cultures; mean values ± SEM). The number of cleaved caspase3-positive cells in Ep400-deficient cells transduced with control retrovirus was set to 1. Statistical significance was determined by two-tailed Student's *t*-test ($^{**}P \leq 0.01$).

teins between GST and conserved Sox10 domains (Figure 8B) and polypeptides corresponding to functional Ep400 domains (Figure 8C). A polypeptide consisting of dimerization and DNA-binding HMG-domain (38), but not the K2 or C-terminal transactivation domains of Sox10 interacted with Ep400 (Figure 8B and D). In Ep400, Sox10 binding mapped to the HSA and the SANT domains, but not to the N-terminal region, the ATPase domain or the glutamine-rich C-terminal region (Figure 8C and D). Given their ability to interact and both bind to ECR9, Sox10 and Ep400 may thus cooperate to activate *Myrf* expression during OL differentiation.

To analyze whether *Myrf* activation constitutes an essential aspect of Ep400 function in OL differentiation, we isolated OPCs from *Ep400ΔC* mice, transduced them with control or Myrf-expressing retrovirus and subjected them to differentiating conditions. Intriguingly, very few Ep400-deficient OPCs developed into Mbp-expressing OLs in culture independent of whether they remained uninfected or transduced with tdTomato-expressing control retrovirus. In contrast, transduction with Myrf- and tdTomato-

expressing retrovirus led to a strong increase of Mbp-positive cells in culture (Figure 8E and F). However, rates of apoptosis remained high in Ep400-deficient cells even in the presence of Myrf (Figure 8G). This argues that ectopic Myrf can rescue the differentiation but not the survival defect in Ep400-deficient OLs.

Ep400 is not required for myelin maintenance

To analyze whether Ep400 is also required at late oligodendroglial stages, we combined the *Ep400*^{fl} allele with *Mog*$^{i\text{-}Cre}$. In the resulting *Ep400ΔM* mice Ep400 deletion occurs substantially after the induction of terminal differentiation and myelin gene expression in already myelinating OLs (39). Cells during the early stages of terminal differentiation and myelination still contain Ep400. Ep400 deletion in *Ep400ΔM* mice was very efficient and amounted to 93 ± 1% at P32 and 85 ± 5% at P60 as evident from immunohistochemistry (Figure 9A and B). Despite efficient deletion, *Ep400ΔM* mice had normal numbers of Olig2- and Sox10-positive oligodendroglial cells at P32 and P60 (Figure 9C–J). Myrf, Mbp and *Plp1* as markers of the myelinated state were similarly expressed in *Ep400ΔM* and control mice (Figure 9K–V). Proliferation and survival rates were also comparable (Figure 9W and X). We conclude that Ep400 is dispensable during later stages of myelination and for myelin homeostasis.

DISCUSSION

By specifically deleting Ep400 as the central ATP-hydrolyzing subunit, we show here for the first time that the TIP60/EP400 chromatin remodeling complex is an important component of the OL differentiation program. Its activity is not required for oligodendroglial specification and lineage progression at embryonic times but becomes important during terminal differentiation and the active phase of the myelination process. Intriguingly, Ep400 activity again becomes dispensable in late differentiating and mature OLs in which the myelination program is already established.

During the phase when terminal differentiation starts and myelination is induced, the chromatin landscape undergoes the most dramatic changes in oligodendroglial cells as for instance evident by the strong increase in heterochromatinization and nuclear condensation (12). We conclude that Ep400 is involved in implementing and consolidating these changes. In addition, the gene regulatory network has to be adjusted at this time to trigger terminal differentiation and myelination programs. In the absence of Ep400, genes coding for proteins of the myelin sheath or involved in lipid metabolism exhibit decreased expression. While this may be in part a direct effect on the expression of the various genes, we also found evidence for an impact of Ep400 on the oligodendroglial gene regulatory network (Figure 9Y). An essential network component with reduced expression after Ep400 loss is the transcription factor Myrf (37). We found that Ep400 binds specifically to promoter and enhancer regions of the *Myrf* gene already prior to its induction and upon differentiation elicits changes in the H2A.Z localization pattern on the promoter. This indicates that Ep400 directly influences *Myrf* expression and thereby adjusts overall network activity for OL differentiation and myelination. The biological relevance of the Ep400 effect on *Myrf* expression is further supported by the ability of ectopic Myrf to rescue the differentiation defect in cultured Ep400-deficient OLs.

Myrf has previously been shown to be required for induction as well as maintenance of myelination and once induced, Myrf expression persists in OLs (37,40). Persistent Myrf expression was also observed in OLs of *Ep400ΔM* mice. This argues that Ep400 is important for Myrf induction, but not for maintenance of Myrf expression. Several reasons can be envisaged for this. For one, Ep400-dependent effects such as chromatin modifications may only be needed once and stably remain in place thereafter. Alternatively, Myrf expression may be differentially regulated during induction and maintenance phase because of different promoter usage or alternative splicing. This remains to be clarified in future studies.

We have previously reported a role for Sox10 in Myrf expression that resembles the function of Ep400 (28). Both Sox10 and Ep400 bind to the ECR9 enhancer and physically interact with each other. This argues that both the remodeler and the transcription factor cooperate in the activation of Myrf expression. Other pairs of chromatin remodeler and transcription factors have already been described such as Brg1 and Olig2 in the induction of Sox10 during oligodendroglial specification (6), Chd7 and Sox2 in the regulation of cell cycle genes in OPCs (9) or Chd7 and Sox10 in the induction of genes with relevance for myelinogenesis in OLs (8). In all these cases, it is assumed that it is the transcription factor that recruits the chromatin remodeler to specific genes in a cell type-specific manner. In contrast to Ep400, Sox10 was found on ECR9 only in OLs and not yet in OPCs. Ep400 binding to ECR9 therefore precedes Sox10 binding. This argues that recruitment of Ep400 to the *Myrf* gene is not through Sox10. Instead, Ep400 may help to recruit Sox10 and this may represent a mechanism by which Ep400 influences gene expression independent of its chromatin remodeling activity.

In addition to its effects on terminal differentiation and myelination programs, Ep400 was also required for OL survival. Increased apoptosis and decreased oligodendroglial cell numbers were only observed postnatally at times when the differentiation defect was already visible for several days in *Ep400ΔC* mice. Despite the overall decrease in oligodendroglial cells, OPC numbers and proliferation rates remained constant at least during the first month of life. This indicates that the requirement of Ep400 for survival is restricted to differentiating OLs. The observed later increase in the number of OPCs and their proliferation rates likely represents a compensatory mechanism for the persistent continuous OL loss. Interestingly, *Ep400ΔM* mice with an Ep400 deletion in mature OL also did not show increased apoptosis (Figure 9X) indicating that Ep400 enhances OL survival specifically during the early phase of differentiation and myelination. In mice with oligodendroglial Chd7 deletion, survival is selectively affected at the OPC stage (10). This argues that oligodendroglial survival depends on other chromatin remodelers at different developmental times.

Our RNA-Seq data unraveled another function of Ep400 by detecting alterations in DNA damage response and double-strand break repair in *Ep400ΔC* mice. Increased

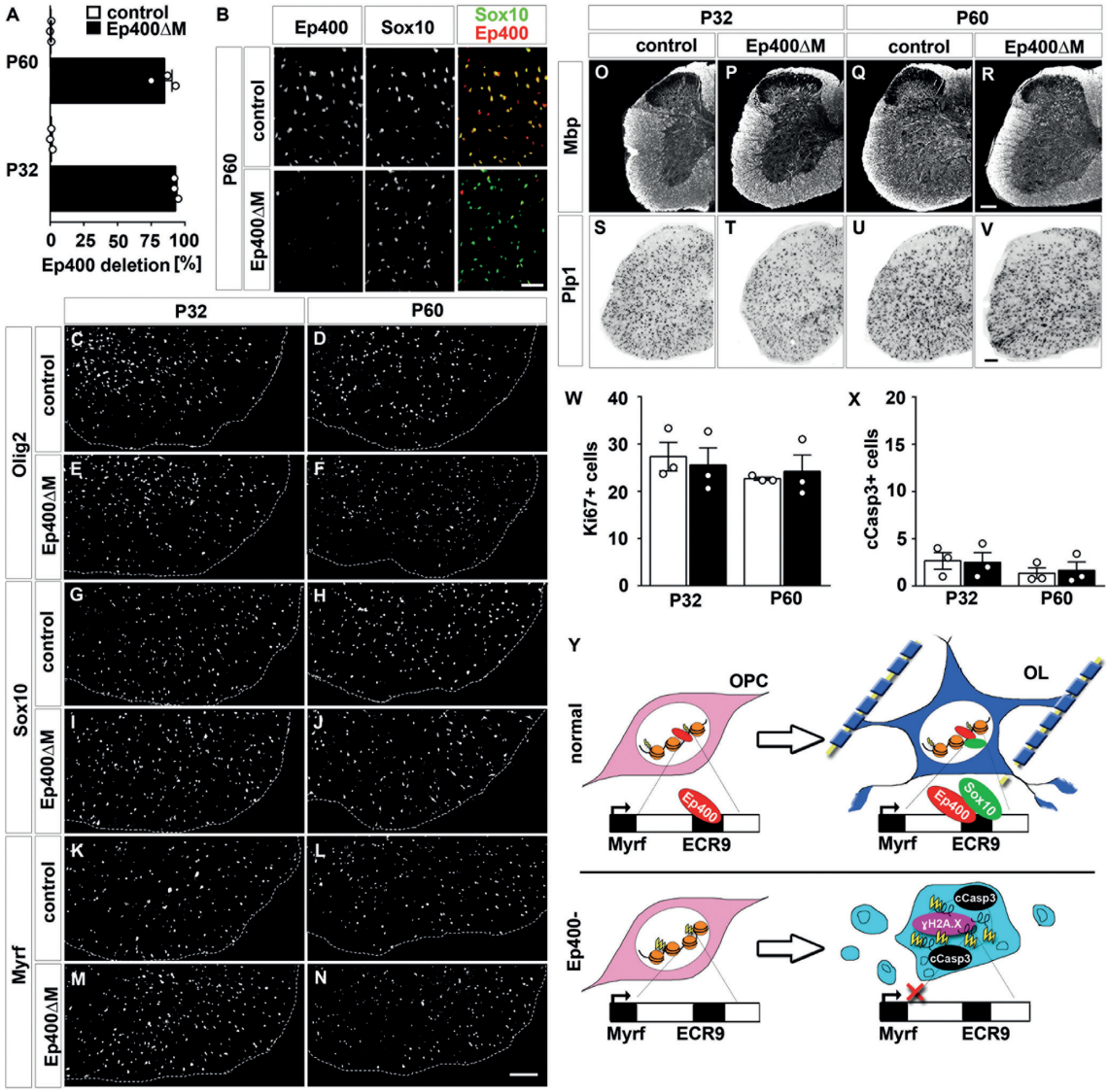

Figure 9. Unaffected oligodendroglial cells in *Ep400ΔM* mice despite efficient Ep400 deletion. (**A**, **B**) Quantification of Ep400-negative oligodendroglial cells in $Ep400^{fl/fl}$ *Mog::iCre* (*Ep400ΔM*, black bars) mice as determined by Ep400 immunohistochemistry at P32 and P60 relative to age-matched controls (white bars). Oligodendroglial cells were identified by Sox10 staining. Three embryos per genotype were used for quantification, counting three separate sections each. Mean relative numbers ± SEM per section are presented. Representative immunohistochemical stainings are shown (Sox10 in green and Ep400 in red). (**C–V**) Analysis of oligodendroglial marker expression by immunohistochemistry (C–R) and *in situ* hybridization (S–V) on transverse spinal cord sections of control (C, D, G, H, K, L, O, Q, S, U) and $Ep400^{fl/fl}$ $Mog^{i\text{-}Cre/+}$ (E, F, I, J, M, N, P, R, T, V) mice at P32 (C, E, G, I, K, M, O, P, S, T) and P60 (D, F, H, J, L, N, Q, R, U, V). Antibodies were directed against Olig2 (C–F), Sox10 (G–J), Myrf (K–N), and Mbp (O–R). Riboprobes recognized *Plp1* mRNA (S–V). Scale bars: 50 μm (B), 100 μm (N, R, V). (**W**, **X**) Quantifications of Ki67 (W) and cleaved caspase 3 (cCasp3, X) for control (white bars) and *Ep400ΔM* (black bars) spinal cord at P32 and P60 ($n = 3$ mice for each genotype, counting three separate sections). Mean cell numbers ± SEM per section are presented. No statistically significant differences were detected. (**Y**) Proposed model of Ep400 function during oligodendroglial differentiation and myelination by preventing DNA damage-induced apoptosis and Myrf-dependent induction of the myelination program in cooperation with Sox10.

γH2A.X labeling of Ep400-deficient OLs in culture confirmed these changes. As unrepaired DNA damage is a well-known apoptotic stimulus, it is reasonable to assume that the pro-survival effect of Ep400 in differentiating OLs is caused by a role in DNA repair. Such function has been described for SWR-type chromatin remodeling complexes in cultured cells (41) but has never been reported in multicellular organisms *in vivo*. The fact that the DNA repair function of Ep400 becomes evident at a time when chromatin structure changes most dramatically in OLs may indicate that the genome is particularly prone to damage during this period.

Interestingly, ectopically expressed Myrf was unable to increase survival in Ep400-deficient OLs arguing that Ep400 exerts its pro-survival function in these cells independent of Myrf.

Increased cell death had also been observed in a previous study where Ep400 had been deleted in the adult hematopoietic system (18) suggesting that the pro-survival function of Ep400 may be more general. The same study also found proliferation defects and showed an impaired expression of many cell cycle regulatory genes in Ep400-deficient mouse embryonic fibroblasts. Intriguingly, pro-

liferation was unchanged in the oligodendroglial cell lineage arguing that proliferative functions of Ep400 may be less general and dependent on the cell-type or tissue under study.

The TIP60/EP400 complex is the first chromatin remodeler of the INO80/SWR subfamily that has been studied in the CNS and in the OL lineage following deletion of its central energy supplying Ep400 subunit. Redundancy within this subfamily is fairly limited as Srcap is the only other SWR-type chromatin remodeling complex in vertebrates and as SWR and INO80 chromatin remodeling complexes have largely different roles *in vitro* (2,3). According to published RNA-Seq data (34) Srcap expression levels in oligodendroglial cells furthermore appear to be very low. This indicates that most of the functions exerted by SWR chromatin remodeling complexes in oligodendroglial cells require Ep400 and that there is little functional compensation within the subfamily after its loss.

Our transcriptomic studies did not reveal any evidence for a close functional relationship between Ep400 and Brg1 or Chd7. This conclusion was also supported from findings in compound mouse mutants. *Ep400ΔC* mice with additional loss of one *Brg1* allele phenotypically resembled *Ep400ΔC* mice. We therefore assume largely separate functions for TIP60/EP400 as compared to BAF and CHD-type complexes on a global scale. This in turn predicts little compensatory capabilities and may explain the severity of the phenotypic defects in *Ep400ΔC* mice.

In summary, our data show that Ep400-dependent SWR chromatin remodeling activity is an essential driver of the chromatin changes that occur during OL differentiation and is required for execution of the myelination program (Figure 9Y). They also point to Ep400 as a pro-survival factor that safeguards against DNA damage or helps in its repair during the same phase. As both functions are also useful for remyelination after injury or demyelination, Ep400 activity may present a suitable target for therapeutic strategies in myelin repair.

DATA AVAILABILITY

All data generated or analyzed during this study are included in this published article and its supplementary file or have been deposited in the GEO database (accession number: GSE119127).

SUPPLEMENTARY DATA

Supplementary Data are available at NAR Online.

ACKNOWLEDGEMENTS

We thank Drs F. Constantini, D. Metzger, K.-A. Nave, W.D. Richardson, G. Schütz and A. Waisman for providing mouse lines. M. Schimmel is acknowledged for expert technical assistance and E. Sock for critically reading the manuscript.

Authors contributions: M.W. conceived and supervised the study. O.E., F.F. and M.W. designed the experiments. O.E., F.F., M.K. and E.R.T. performed the experiments. R.F. and T.F. provided important reagents and materials. O.E., F.F., M.K., E.R.T. and M.W. analyzed the data. O.E., F.F. and M.W. wrote the manuscript.

FUNDING

Deutsche Forschungsgemeinschaft [We1326/14, GRK2162 to M.W.]. Funding for open access charge: Deutsche Forschungsgemeinschaft & Universität Erlangen-Nürnberg.

Conflict of interest statement. None declared.

REFERENCES

1. Küspert,M. and Wegner,M. (2016) SomethiNG 2 talk about - Transcriptional regulation in embryonic and adult oligodendrocyte precursors. *Brain Res.*, **1638**, 167–182.
2. Hota,S.K. and Bruneau,B.G. (2016) ATP-dependent chromatin remodeling during mammalian development. *Development*, **143**, 2882–2897.
3. Venkatesh,S. and Workman,J.L. (2015) Histone exchange, chromatin structure and the regulation of transcription. *Nat. Rev. Mol. Cell Biol.*, **16**, 178–189.
4. Bartholomew,B. (2014) Regulating the chromatin landscape: structural and mechanistic perspectives. *Annu. Rev. Biochem.*, **83**, 671–696.
5. Bischof,M., Weider,M., Küspert,M., Nave,K.A. and Wegner,M. (2015) Brg1-Dependent chromatin remodelling is not essentially required during oligodendroglial differentiation. *J. Neurosci.*, **35**, 21–35.
6. Yu,Y., Chen,Y., Kim,B., Wang,H., Zhao,C., He,X., Liu,L., Liu,W., Wu,L.M., Mao,M. *et al.* (2013) Olig2 targets chromatin remodelers to enhancers to initiate oligodendrocyte differentiation. *Cell*, **152**, 248–261.
7. Matsumoto,S., Banine,F., Struve,J., Xing,R., Adams,C., Liu,Y., Metzger,D., Chambon,P., Rao,M.S. and Sherman,L.S. (2006) Brg1 is required for murine neural stem cell maintenance and gliogenesis. *Dev. Biol.*, **289**, 372–383.
8. He,D., Marie,C., Zhao,C., Kim,B., Wang,J., Deng,Y., Clavairoly,A., Frah,M., Wang,H., He,X. *et al.* (2016) Chd7 cooperates with Sox10 and regulates the onset of CNS myelination and remyelination. *Nat. Neurosci.*, **19**, 678–689.
9. Doi,T., Ogata,T., Yamauchi,J., Sawada,Y., Tanaka,S. and Nagao,M. (2017) Chd7 collaborates with Sox2 to regulate activation of oligodendrocyte precursor cells after spinal cord injury. *J. Neurosci.*, **37**, 10290–10309.
10. Marie,C., Clavairoly,A., Frah,M., Hmidan,H., Yan,J., Zhao,C., Van Steenwinckel,J., Daveau,R., Zalc,B., Hassan,B. *et al.* (2018) Oligodendrocyte precursor survival and differentiation requires chromatin remodeling by Chd7 and Chd8. *Proc. Natl. Acad. Sci. U.S.A.*, **115**, E8246–E8255.
11. Zhao,C., Dong,C., Frah,M., Deng,Y., Marie,C., Zhang,F., Xu,L., Ma,Z., Dong,X., Lin,Y. *et al.* (2018) Dual requirement of CHD8 for chromatin landscape establishment and histone methyltransferase recruitment to promote CNS myelination and repair. *Dev. Cell*, **45**, 753–768.
12. Mori,S. and Leblond,C.P. (1970) Electron microscopic identification of three classes of oligodendrocytes and a preliminary study of their proliferative activity in the corpus callosum of young rats. *J. Comp. Neurol.*, **139**, 1–28.
13. Kusch,T., Florens,L., Macdonald,W.H., Swanson,S.K., Glaser,R.L., Yates,J.R. 3rd, Abmayr,S.M., Washburn,M.P. and Workman,J.L. (2004) Acetylation by Tip60 is required for selective histone variant exchange at DNA lesions. *Science*, **306**, 2084–2087.
14. Mizuguchi,G., Shen,X., Landry,J., Wu,W.H., Sen,S. and Wu,C. (2004) ATP-driven exchange of histone H2AZ variant catalyzed by SWR1 chromatin remodeling complex. *Science*, **303**, 343–348.
15. Pradhan,S.K., Su,T., Yen,L., Jacquet,K., Huang,C., Cote,J., Kurdistani,S.K. and Carey,M.F. (2016) EP400 deposits H3.3 into promoters and enhancers during gene activation. *Mol. Cell*, **61**, 27–38.

16. Lu,P.Y., Levesque,N. and Kobor,M.S. (2009) NuA4 and SWR1-C: two chromatin-modifying complexes with overlapping functions and components. *Biochem. Cell Biol.*, **87**, 799–815.
17. Fazzio,T.G., Huff,J.T. and Panning,B. (2008) An RNAi screen of chromatin proteins identifies Tip60-p400 as a regulator of embryonic stem cell identity. *Cell*, **134**, 162–174.
18. Fujii,T., Ueda,T., Nagata,S. and Fukunaga,R. (2010) Essential role of p400/mDomino chromatin-remodeling ATPase in bone marrow hematopoiesis and cell-cycle progression. *J. Biol. Chem.*, **285**, 30214–30223.
19. Ueda,T., Watanabe-Fukunaga,R., Ogawa,H., Fukuyama,H., Higashi,Y., Nagata,S. and Fukunaga,R. (2007) Critical role of the p400/mDomino chromatin-remodeling ATPase in embryonic hematopoiesis. *Genes Cells*, **12**, 581–592.
20. Tronche,F., Kellendonk,C., Kretz,O., Gass,P., Anlag,K., Orban,P.C., Bock,R., Klein,R. and Schütz,G. (1999) Disruption of the glucocorticoid receptor gene in the nervous system results in reduced anxiety. *Nat. Genet.*, **23**, 99–103.
21. Matsuoka,T., Ahlberg,P.E., Kessaris,N., Iannarelli,P., Dennehy,U., Richardson,W.D., McMahon,A.P. and Koentges,G. (2005) Neural crest origins of the neck and shoulder. *Nature*, **436**, 347–355.
22. Stolt,C.C., Schlierf,A., Lommes,P., Hillgärtner,S., Werner,T., Kosian,T., Sock,E., Kessaris,N., Richardson,W.D., Lefebvre,V. *et al.* (2006) SoxD proteins influence multiple stages of oligodendrocyte development and modulate SoxE protein function. *Dev. Cell*, **11**, 697–710.
23. Lappe-Siefke,C., Goebbels,S., Gravel,M., Nicksch,E., Lee,J., Braun,P.E., Griffiths,I.R. and Nave,K.A. (2003) Disruption of Cnp1 uncouples oligodendroglial functions in axonal support and myelination. *Nat. Genet.*, **33**, 366–374.
24. Hövelmeyer,N., Hao,Z., Kranidioti,K., Kassiotis,G., Buch,T., Frommer,F., von Hoch,L., Kramer,D., Minichiello,L., Kollias,G. *et al.* (2005) Apoptosis of oligodendrocytes via Fas and TNF-R1 is a key event in the induction of experimental autoimmune encephalomyelitis. *J. Immunol.*, **175**, 5875–5884.
25. Sumi-Ichinose,C., Ichinose,H., Metzger,D. and Chambon,P. (1997) SNF2beta-BRG1 is essential for the viability of F9 murine embryonal carcinoma cells. *Mol. Cell Biol.*, **17**, 5976–5986.
26. Srinivas,S., Watanabe,T., Lin,C.S., William,C.M., Tanabe,Y., Jessell,T.M. and Costantini,F. (2001) Cre reporter strains produced by targeted insertion of EYFP and ECFP into the ROSA26 locus. *BMC Dev. Biol.*, **1**, 4.
27. McCarthy,K.D. and DeVellis,J. (1980) Preparation of separate astroglial and oligodendroglial cell cultures from rat cerebral tissue. *J. Cell Biol.*, **85**, 890–902.
28. Hornig,J., Fröb,F., Vogl,M.R., Hermans-Borgmeyer,I., Tamm,E.R. and Wegner,M. (2013) The transcription factors Sox10 and myrf define an essential regulatory network module in differentiating oligodendrocytes. *PLoS Genet.*, **9**, e1003644.
29. Maka,M., Stolt,C.C. and Wegner,M. (2005) Identification of Sox8 as a modifier gene in a mouse model of Hirschsprung disease reveals underlying molecular defect. *Dev. Biol.*, **277**, 155–169.
30. Kuhlbrodt,K., Herbarth,B., Sock,E., Hermans-Borgmeyer,I. and Wegner,M. (1998) Sox10, a novel transcriptional modulator in glial cells. *J. Neurosci.*, **18**, 237–250.
31. Weider,M., Küspert,M., Bischof,M., Vogl,M.R., Hornig,J., Loy,K., Kosian,T., Müller,J., Hillgärtner,S., Tamm,E.R. *et al.* (2012) Chromatin-remodeling factor Brg1 is required for Schwann cell differentiation and myelination. *Dev. Cell*, **23**, 193–201.
32. Jagasia,R., Steib,K., Englberger,E., Herold,S., Faus-Kessler,T., Saxe,M., Gage,F.H., Song,H. and Lie,D.C. (2009) GABA-cAMP response element-binding protein signaling regulates maturation and survival of newly generated neurons in the adult hippocampus. *J. Neurosci.*, **29**, 7966–7977.
33. Stolt,C.C., Lommes,P., Sock,E., Chaboissier,M.-C., Schedl,A. and Wegner,M. (2003) The Sox9 transcription factor determines glial fate choice in the developing spinal cord. *Genes Dev.*, **17**, 1677–1689.
34. Zhang,Y., Chen,K., Sloan,S.A., Bennett,M.L., Scholze,A.R., O'Keeffe,S., Phatnani,H.P., Guarnieri,P., Caneda,C., Ruderisch,N. *et al.* (2014) An RNA-sequencing transcriptome and splicing database of glia, neurons, and vascular cells of the cerebral cortex. *J. Neurosci.*, **34**, 11929–11947.
35. Finzsch,M., Stolt,C.C., Lommes,P. and Wegner,M. (2008) Sox9 and Sox10 influence survival and migration of oligodendrocyte precursors in the spinal cord by regulating PDGF receptor {alpha} expression. *Development*, **135**, 637–646.
36. Natarajan,C. and Takeda,K. (2017) Regulation of various DNA repair pathways by E3 ubiquitin ligases. *J. Cancer Res. Ther.*, **13**, 157–169.
37. Emery,B., Agalliu,D., Cahoy,J.D., Watkins,T.A., Dugas,J.C., Mulinyawe,S.B., Ibrahim,A., Ligon,K.L., Rowitch,D.H. and Barres,B.A. (2009) Myelin gene regulatory factor is a critical transcriptional regulator required for CNS myelination. *Cell*, **138**, 172–185.
38. Weider,M., Reiprich,S. and Wegner,M. (2013) Sox appeal - Sox10 attracts epigenetic and transcriptional regulators in myelinating glia. *Biol. Chem.*, **394**, 1583–1593.
39. Turnescu,T., Arter,J., Reiprich,S., Tamm,E.R., Waisman,A. and Wegner,M. (2018) Sox8 and Sox10 jointly maintain myelin gene expression in oligodendrocytes. *Glia*, **66**, 279–294.
40. Koenning,M., Jackson,S., Hay,C.M., Faux,C., Kilpatrick,T.J., Willingham,M. and Emery,B. (2012) Myelin gene regulatory factor is required for maintenance of myelin and mature oligodendrocyte identity in the adult CNS. *J. Neurosci.*, **32**, 12528–12542.
41. Morrison,A.J. and Shen,X. (2009) Chromatin remodelling beyond transcription: the INO80 and SWR1 complexes. *Nat. Rev. Mol. Cell Biol.*, **10**, 373–384.